lation it remains to be seen what the effects will be when the starting model contains large intrinsic errors. Moreover, for structures successfully refined at high resolution by classical procedures, the occurrence of large errors is most unlikely, and these structures are therefore good starting points to study the anisotropy and anharmonicity of the atomic distributions in the molecule by the method we present.

Time-averaged crystallographically restrained MD shows that phospholipase A_2 is more flexible than single site isotropic models obtained by classical crystallographic refinement techniques would suggest. Large deviations from the main conformation are observed, and these are likely to be important for the functioning of the molecule. Time-averaged crystallographically restrained MD, when applied to structure refinement, allows for more mobility and better searching of the conformational space, in comparison to least-squares methods and MD refinement procedures (*5, 6*), and provides a more complete representation of a biomacromolecule by calculating the ensemble of structures based on the experimental data. Accurate knowledge of molecular dynamics may prove useful in various fields of biochemistry.

REFERENCES AND NOTES

1. B. Howlin, D. S. Moss, G. W. Harris, *Acta Crystallogr. A* **45**, 851 (1989).
2. J. Kuriyan, G. A. Petsko, R. M. Levy, M. Karplus, *J. Mol. Biol.* **190**, 227 (1986).
3. W. F. van Gunsteren, H. J. C. Berendsen, J. Hermans, W. G. J. Hol, J. P. M. Postma, *Proc. Natl. Acad. Sci. U.S.A.* **80**, 4315 (1983).
4. W. F. van Gunsteren and H. J. C. Berendsen, GROningen MOlecular Simulation (GROMOS) library manual, BIOMOS Biomolecular Software (Laboratory of Physical Chemistry, University of Groningen, Groningen, 1987).
5. A. T. Brünger, J. Kuriyan, M. Karplus, *Science* **235**, 458 (1987).
6. M. Fujinaga, P. Gros, W. F. van Gunsteren, *J. Appl. Crystallogr.* **22**, 1 (1989).
7. A. E. Torda, R. M. Scheek, W. F. van Gunsteren, *Chem. Phys. Lett.* **157**, 289 (1989).
8. ———, *J. Mol. Biol.*, in press.
9. W. A. Pieterson, J. C. Vidal, J. J. Volwerk, G. H. de Haas, *Biochemistry* **13**, 1455 (1974).
10. B. W. Dijkstra, K. H. Kalk, W. G. J. Hol, J. Drenth, *J. Mol. Biol.* **147**, 97 (1981).
11. B. W. Dijkstra, J. Drenth, K. H. Kalk, *Nature* **289**, 604 (1981).
12. E. A. Dennis, *The Enzymes*, P. D. Boyer, Ed. (Academic Press, New York, 1983), vol. 16, pp. 307–353.
13. R. Renetseder, S. Brunie, B. W. Dijkstra, J. Drenth, P. B. Sigler, *J. Biol. Chem.* **260**, 11627 (1985).
14. The GROMOS (*4*)–MDXREF (*6*) program was adjusted according to Eqs. 1 and 2. For this purpose Eq. 2 was rewritten as: $\langle \mathbf{F}_c(\mathbf{s})\rangle_{t'} = \exp\{-\Delta t/\tau_x\}\langle \mathbf{F}_c\rangle_{t'-\Delta t} + (1 - \exp\{-\Delta t/\tau_x\}\mathbf{F}_c^{t'}$ (where Δt is the time step in the simulation). This equation is equivalent to Eq. 2 when $t' >> \tau_x$. The simulation was performed in vacuo with all protein atoms and 106 crystal water molecules of $BPLA_2$. The GROMOS 37D4 force field of (*4*) was used with the SHAKE algorithm to constrain the bond lengths (*15*) and with time steps of 2 fs. From $t = 0$ ps to 16 ps the individual isotropic temperature factors of each atom were gradually reduced to 1 Å^2 for all atoms, while τ_x was increased from 0 to 4 ps. At $t = 20$ ps τ_x was increased to 8 ps and at $t = 26$ ps to $\tau_x = 16$ ps. Up to $t = 28$ ps the temperature was coupled to a bath (*16*) of 150 K with a temperature-relaxation time, τ_T, of 0.012 ps; afterward the bath temperature was set to 200 K. During the whole run σ_x was kept at 140 (arbitrary units), which is roughly equivalent to $(\langle(|\mathbf{F}_o| - |\mathbf{F}_c|)^2\rangle^{1/2})$ at $t = 0$ ps. All of the x-ray data between 8.0 and 1.7 Å resolution with $|\mathbf{F}_o| > \sigma_{\mathbf{F}o}$ were used in the calculations. Heating was observed in the presented simulation. The amount of heating depends on the magnitude of τ_x; for $\tau_x = 4$ ps, $\Delta T = 108$ K, for $\tau_x = 8$ ps, $\Delta T = 56$ K, and for $\tau_x = 16$ ps, $\Delta T = 30$ K, where ΔT is defined as $\langle T\rangle - T_{\mathrm{bath}}$. The average potential energy of the simulated system observed from $t = 40$ to 80 ps is -4.52×10^3 kJ/mole, compared with -5.31×10^3 kJ/mole for an unrestrained simulation of $BPLA_2$ in vacuo at 300 K. A related measure is the average root-mean-square deviations from standard geometry of the structures from the ensemble, which are 0.015 Å for bond lengths, 4.2° for bond angles, and 28° for torsion angles, as calculated by the program TNT (*17*) from a subset of structures taken at 4-ps intervals from the ensemble.
15. J. P. Ryckaert, G. Ciccotti, H. J. C. Berendsen, *J. Comput. Phys.* **23**, 327 (1977).
16. H. J. C. Berendsen, J. P. M. Postma, W. F. van Gunsteren, A. Dinola, J. R. Haak, *J. Chem. Phys.* **81**, 3684 (1984).
17. D. E. Tronrud, L. ten Eyck, B. W. Matthews, *Acta Crystallogr. A* **43**, 489 (1987).
18. O. P. Kuipers *et al.*, *Science* **244**, 82 (1989).
19. M. P. Allen and D. J. Tildesley, *Computer Simulation of Liquids* (Clarendon, Oxford, 1987).
20. J. Hermans, H. J. C. Berendsen, W. F. van Gunsteren, J. P. M. Postma, *Biopolymers* **23**, 1513 (1984).
21. A. T. Brünger, *J. Mol. Biol.* **203**, 803 (1988).
22. M. G. Vincent and J. P. Priestle, *J. Appl. Crystallogr.* **18**, 185 (1985).

23. We thank A. E. Torda and M. Fujinaga for helpful and stimulating discussions and B. W. Dijkstra for generously supplying the x-ray diffraction data of phospholipase. Supported by the Dutch Foundation for Chemical Research (SON) with financial aid from the Dutch Organization for Scientific Research (NWO).

24 April 1990; accepted 25 July 1990

Possible Early Pennsylvanian Ancestor of the Cycadales

Richard L. Leary

A specimen of *Lesleya*, previously known only as isolated sterile foliage, has been found with two rows of ovule-bearing receptacles on opposite sides of the petiole. This specimen is from the Lower Pennsylvanian (Namurian B or C) of western Illinois. The fertile portion of this specimen is similar to *Phasmatocycas kansana* Mamay from the Lower Permian of Kansas and Texas, which Mamay interpreted as an ancestral form to cycads. *Phasmatocycas* was found attached to the base of *Taeniopteris* by Gillespie and Pfefferkorn. The foliar portions, *Lesleya* and *Taeniopteris*, have many features in common; the major morphologic difference is curvature of the veins. *Lesleya* and its attached fertile petiole are proposed as ancestors of *Taeniopteris* and *Phasmatocycas*, and ultimately, the ancestors of modern cycads. This extends the age of known precursors of cycads back from the Early Permian to Early Pennsylvanian (about 320 million years ago), approximately 35 million years earlier.

During the past 20 years, several fossil discoveries have shed light on the question of the origin of cycads. Delevoryas (*1*) suggested an origin within the medullosan pteridosperms. He suggested that cycads and cycadeoids were derived from slender plants bearing compound leaves. He (*2*) compared the Pennsylvanian pinnately compound *Eremopteris zamioides* (Bertrand) Kidston and Permian *Tinsleya texana* Mamay to compound early cycad foliage.

Mamay (*3*), on the other hand, in describing *Archaeocycas* and *Phasmatocycas*, suggested that cycads were derived from plants with entire leaves. This was borne out by Gillespie and Pfefferkorn (*4*) who found *Taeniopteris* attached to *Phasmatocycas*. The material described here provides additional evidence that cycads were derived from plants with entire leaves and that compound leaves were derived as suggested by Mamay [figure 11 of (*5*)].

Several sites in western Illinois have yielded significant information about Early Pennsylvanian nonswamp floras, both on their overall composition and on individual taxa within the floras (*6, 7*). The Allied Stone Company quarry in Milan, Illinois, (*8*) has been a major collecting site for nearly 15 years and continues to produce new species and genera as well as new data on known taxa.

Specimens described here were collected from Lower Pennsylvanian sedimentary rocks which fill channels eroded in the Devonian Cedar Valley Limestone (*8*). The fossil-bearing strata consist of shale, siltstone, sandstone, and occasional thin conglomerate.

Department of Geology, Illinois State Museum, Springfield, IL 61706.

Stratigraphically, the age of the fossil-bearing shale is difficult to determine. The shale is underlain by upper Middle Devonian Cedar Valley Limestone and overlain by basal Atokan sandstone, probably the Babylon Sandstone Member of the Abbott Formation.

The age of the fossil-bearing beds can be determined through the megaflora as probably Namurian B with a possibility of a Namurian C age (*6*, *8*). This result is based on concurrently occurring taxa, and the uncertainty arises from the incomplete knowledge of the range of a few species. Palynological investigations also indicate a Namurian B or C age (*11*).

Among the abundant and well-preserved fossil plants from the Lower Pennsylvanian strata of the Allied quarry deposits are *Lesleya*, *Megalopteris*, *Lacoea*, *Palaeopteridium*, *Alethopteris*, *Sphenopteris*, *Cordaites*, *Mesocalamites*, and *Lepidodendron*. These fossils represent plants growing in both wet and drier, well-drained areas.

Specimens of several previously undescribed fructifications have been found in the Allied quarry deposits. Among these are stout, coalified axes with two rows of ovules, similar to *Phasmatocycas* Mamay (*3*). These compression and impression fossils represent the earliest known ancestors of modern cycads and further link this group to early pteridosperms.

Mamay (*3*, *9*, *10*) discussed fossil evidence for a Late Paleozoic origin of cycads and named two new genera of megasporophylls, *Archaeocycas* and *Phasmatocycas*, from lower Leonardian strata of Kansas and Texas. He interpreted these taxa as links in the cycadalean lineage.

Mamay (*11*) postulated that *Phasmatocycas* fertile axis was borne at the base of *Taeniopteris*. This was shown to be correct by Gillespie and Pfefferkorn (*4*) who found attached *Phasmatocycas* and *Taeniopteris*.

Specimens described by Mamay (*3*, *5*, *9*, *10*) are from lower Leonardian (Lower Permian) rocks of Texas, Kansas, and Oklahoma. The specimens described by Gillespie and Pfefferkorn (*4*) are from the Wellington Formation of Leonardian age in Kansas.

Specimens from Illinois have ovuliferous receptacles arranged in two rows on opposite sides of the axis and are similar to *Phasmatocycas* Mamay. Ovules are borne in receptacles attached to the petiole of *Lesleya* by broad, stout bases (Figs. 1 and 2). Receptacles are alternate to subopposite. Receptacle bases are decurrent on the petiole, curving outward to terminate nearly perpendicular to the petiole. Like the petiole, the receptacle base is thick, coalified, and coarsely striated. Because the specimens are coalified, it is unclear whether each receptacle bore one or several seeds.

A lamina is present on only one specimen (ISM 417064) (Fig. 1). The attached specimen consists of a fragment of fertile axis 6 cm long and basal portion of a leaf 8 cm long. The leaf is folded so only one half is visible. Based upon venation patterns and details of associated foliage, the leaf is identified as *Lesleya cheimarosa* Leary & Pfefferkorn.

The fertile material consists of seven fragments. Ovuliferous fragments range from 4 cm to 9 cm in length and 10 mm to 18 mm in width. The central axes average 5.5 mm wide, the thick midribs average 1.8 mm wide, and the projecting ovuliferous receptacles average 3 mm long. The coalified axes are up to 1 mm thick. The midrib is characterized by closely spaced longitudinal ribs. The outer ribs depart at a low angle, gradually curving outward into the receptacles.

The taxa described here are so similar that a relation is most likely. However, it is not certain that they were all directly related. They might have represented offshoots of a general lineage that is incompletely known.

Because the Lower Pennsylvanian material from western Illinois predates *Spermopteris* as well as *Phasmatocycas* and *Archaeocycas*, it is possible *Archaeocycas* and *Phasmatocycas* were derived from the form described here. This would mean that *Spermopteris* is not an ancestor of *Phasmatocycas* or *Archaeocycas*.

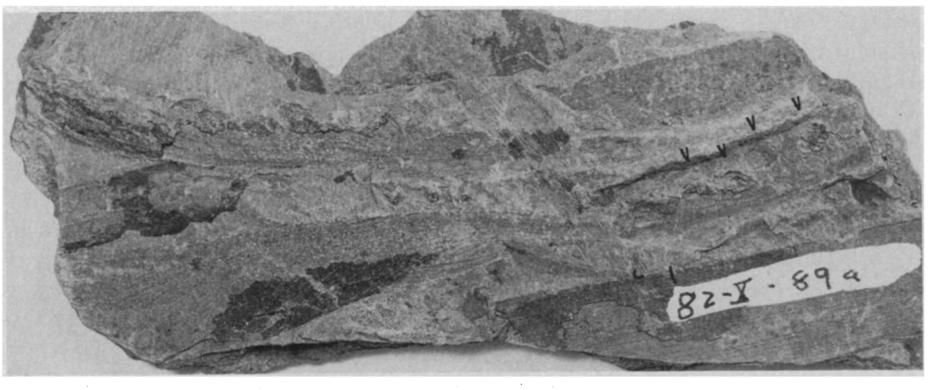

Fig. 1. *Lesleya* with ovule-bearing petiole. Arrowheads indicate receptacles. Sample is 10.8 cm long.

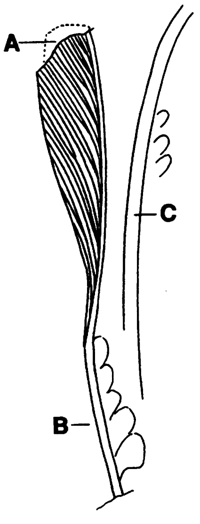

Fig. 2. Drawing of specimen showing (**A**) part of lamina folded under, (**B**) ovules on right side (those on left are not visible), and (**C**) second fertile petiole.

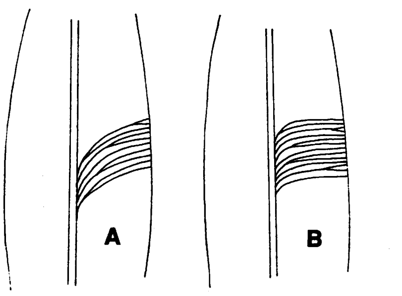

Fig. 3. Venation of (**A**) *Lesleya* and (**B**) *Taeniopteris*.

Another possibility is that a *Spermopteris*-like ancestor existed during the Early Carboniferous. Lower Carboniferous upland floras are even less well known than Upper Carboniferous upland floras, leaving open the question of an earlier existence of *Spermopteris*.

The Illinois material resolves, in part, another question raised by Mamay (*5*, p. 44), the origin of taeniopterid foliage. *Lesleya* and *Taeniopteris* are morphologically similar, and several features have suggested a relation. They differ morphologically in the curvature of the veins (Fig. 3), and a change from arched to perpendicular would not seem unreasonable.

Specimens of *Lesleya* often possess resinous spots similar to the glands reported from *Taeniopteris*. Such glands were reported on *Taeniopteris* specimens associated with *Phasmatocycas* (*5*) and on the fertile specimen described by Gillespie and Pfefferkorn (*4*).

The Illinois specimens of *Lesleya* push the origin of the cycadales from the Early Permian (Leonardian) back to the Early Pennsylvanian (mid-Namurian), approximately 35 million years earlier. The presence of these ancestors in a mesophilous flora which grew on a well-drained extra-basinal surface (*8*) adds further evidence that major evolutionary events occurred outside the peat and alluvial depositional areas in which plants are most often preserved.

REFERENCES AND NOTES

1. T. Delevoryas, *Rev. Palaeobot. Palynol.* **37**, 115 (1982).
2. ———, in *Gondwana Geology, Papers from the Third International Gondwana Symposium*, K. S. W. Campbell, Ed., Canberra, Australia (Australian National Univ. Press, Canberra, 1973), pp. 173–191.
3. S. H. Mamay, *U.S. Geol. Surv. J. Res.* **1**, 687 (1973).
4. W. H. Gillespie and H. W. Pfefferkorn, *Rev. Palaeobot. Palynol.* **49**, 99 (1986).
5. S. H. Mamay, *U.S. Geol. Surv. Prof. Paper* 934 (1976).
6. R. L. Leary and H. W. Pfefferkorn, *Ill. Geol. Surv. Cir.* no. 500 (1977).
7. R. L. Leary, Eighth International Congress on Stratigraphy and Geology of the Carboniferous, Moscow, U.S.S.R., 8 to 13 September 1975 (Nauka, Moscow, 1979), vol. 5, pp. 49–56.
8. ———, *Ill. State Museum Rep. Invest.* no. 37 (1981).
9. S. H. Mamay, *Science* **164**, 295 (1969).
10. ———, Eleventh International Botanical Congress, Seattle, WA, 24 August to 2 September 1969, p. 139 (1969).
11. R. A. Peppers, personal communication.

27 February 1990; accepted 11 June 1990

Cumulate Xenolith in Oahu, Hawaii: Implications for Deep Magma Chambers and Hawaiian Volcanism

GAUTAM SEN AND ROBERT E. JONES

The maximum depth at which large (>1000 km^3) terrestrial mafic magma chambers can form has generally been thought to be the Moho, which occurs at a mean depth of about 35 kilometers beneath the continents and 8 kilometers beneath ocean basins. However, the presence of layers of cumulus magnesium-rich spinel and olivine and intercumulus garnet in an unusual mantle xenolith from Oahu, Hawaii, suggests that this rock is a fragment of a large magma chamber that formed at a depth of about 90 kilometers; Hawaiian shield-building magmas may pond and fractionate in such magma chambers before continuing their ascent. This depth is at or near the base of the 90-million-year-old lithosphere beneath Oahu; thus, rejuvenated stage alkalic magmas containing mantle xenoliths evidently also originate below the lithosphere.

THE DEEPEST LEVEL AT WHICH A large mafic magma chamber can form depends upon the extent of dynamic equilibrium maintained between magma in the chamber and the wall rock and the balance between the deviatoric stress and lithostatic pressure in the mantle where the magma chamber may be located. Magma chambers beneath the ocean ridges are not thought to form below the petrologic Moho, that is, 8 to 10 km below sea level (*1–3*). Seismic studies have been able to detect shallow magma chambers and magma pathways (*4*), but so far have failed to detect deep ($\sim$100 km), large magma chambers beneath the ocean basins, perhaps because of resolution problems. The deepest continental magma chambers are generally thought to occur near the Moho [mean depth $\sim$35 km (*1*)]. Inferences on physical and chemical attributes of terrestrial magma chambers have emerged largely through studies of very large (≥ 1000 km^3) layered intrusions, which represent frozen magma chambers exposed at the surface (*2*). These chambers contain a characteristic rock type, cumulates, which formed by crystallization, accumulation, and segregation of early crystallizing minerals (cumulus) from the magmas (*1*). In this report we suggest that a 90-km-deep magma chamber was present beneath the island of Oahu on the basis of a garnet-bearing cumulate xenolith with layered texture.

The evolution of a typical Hawaiian volcano is marked by four different stages (*5*). In the initial preshield stage, diverse lava types (basanite to tholeiite) erupt. Next, in the shield stage (the main stage), voluminous eruptions of dominantly tholeiitic lavas occur and a caldera develops. The shield stage is usually followed by postshield stage when alkalic basalt (and its differentiates) erupts, fills the collapsed caldera, and forms a thin cap over the shield. In the rejuvenated stage, typically following a period of quiescence and erosion, small volumes of alkalic magmas, many carrying mantle xenoliths, erupt through small vents scattered across the shield.

The eastern part of Oahu is built of a large, tholeiitic shield volcano, known as the Koolau volcano (*5*), that formed 1.8 to 2.7 million years ago. Following cessation of tholeiitic basalt eruption, rejuvenated stage alkalic lavas of the Honolulu Volcanics (HV) erupted 0.3 to 0.6 million years ago through several vents that cut across the volcano (*6*). The HV lavas contain a large number of mantle and crustal xenoliths from a range of depths (*7*); spinel lherzolites are the most abundant upper mantle xenoliths. Garnet-bearing pyroxenites, wehrlites, websterites, and lherzolites are much less common and occur only at the Salt Lake crater at the southwestern flank of the Koolau shield volcano (*8*). The spinel lherzolites are samples of variably enriched mantle lithosphere, and the garnet-bearing rocks are fragments of 60- to 80-km-deep dikes (*9*). Dunite xenoliths are also common, and they represent cumulates that formed in crustal magma chambers (maximum depth $\sim$15 km) of the Koolau volcano (*10*).

We identified a garnet- and spinel-bearing cumulate dunite [sample no. NMNH 114881-8, Dale Jackson Collection, Smithsonian Institution] that was found to occur as an inclusion (xenolith) in HV lavas from the Salt Lake crater. In this rock, discontinuous layers of cumulus spinel grains are interlayered with cumulus olivine grains. Garnet occurs as an intercumulus phase in both layers and in the transition zone (mixed olivine and spinel layer) between adjacent spinel and olivine layers (Fig. 1). Grain sizes of the cumulus phases vary considerably even in a single layer (Fig. 1A). Small (0.25 mm^2) round spinel inclusions are common in olivine grains of the mixed olivine and spinel layer, but olivine grains of the olivine-rich layers are generally free of spinel inclusions. Spinel grains in the spinel layers are coarse to medium size (2 to 7 mm^2) and euhedral to round. Cumulus olivine crystals are mostly rounded, a texture suggesting that they were a reaction relation with the magma. Orthopyroxene forms a thin rim between spinel and garnet, and it may have formed by some late reaction between garnet, spinel, and the magma, such as spinel + magma = garnet + orthopyroxene. Large (2 mm) phlogopite grains also occur interstitially in one area of the xenolith. Whether the phlogopite crystallized from the interstitial melt (that is, primary) or was a later product of metasomatic crystallization is not clear. The petrographic observations suggest that (i) initially spinel and olivine crystallized together as cumulus phases (spinel may have started earlier) and (ii) intercumulus garnet later formed interstitially. The layering may have formed by in situ oscillatory crystallization processes of the type proposed for layered intrusions (*1*). In several continental layered intrusions, such as the Stillwater intrusion, alternate layers of spinel

---

G. Sen, Geology Department, Florida International University, Miami, FL 33199.
R. E. Jones, Department of Earth and Space Sciences, University of California, Los Angeles, CA 90024.